

Dependence of Fanaroff–Riley break of radio galaxies on luminosity and redshift

Ashok K. Singal¹ • Kamlesh Rajpurohit²

Abstract We investigate the dependence of the Fanaroff–Riley (FR) 1/2 dichotomy of radio galaxies on their luminosities and redshifts. Because of a very strong redshift-luminosity correlation (Malmquist bias) in a flux-limited sample, any redshift-dependent effect could appear as a luminosity related effect and vice versa. A question could then arise – do all the morphological differences seen in the two classes (FR 1 and 2 types) of sources, usually attributed to the differences in their luminosities, could as well be primarily a redshift-dependent effect? A sharp break in luminosity, seen among the two classes, could after all reflect a sharp redshift-dependence due to a rather critical ambient density value at some cosmic epoch. A doubt on these lines does not seem to have been raised in past and things have never been examined with this particular aspect in mind. We want to ascertain the customary prevalent view in the literature that the systematic differences in the two broad morphology types of FR 1 and 2 radio galaxies are indeed due to the differences in their luminosities, and not due to a change in redshift. Here we investigate the dependence of FR 1/2 dichotomy of radio galaxies on luminosity and redshift by using the 3CR sample, where the FR 1/2 dichotomy was first seen, supplemented by data from an additional sample (MRC), that goes about a factor of 5 or more deeper in flux-density than the original 3CR sample. This lets us compare sources with similar luminosities but at different redshifts as well as examine sources at similar redshifts but with different luminosities, thereby allowing us a successful separation of the otherwise two

intricately entangled effects. We find that the morphology type is not directly related to redshift and the break between the two types of morphologies seems to depend only upon the radio luminosity.

Keywords galaxies: active — galaxies: evolution — galaxies: nuclei — galaxies: fundamental parameters — radio continuum: galaxies

1 INTRODUCTION

One of the robust correlations in observational astronomy is between the morphology type of radio galaxies and their radio luminosity. First pointed out by Fanaroff and Riley (1974) that there is a very sharp dependence of the morphology type of radio galaxies on the luminosity so that almost all radio galaxies below a luminosity $P_{178} = 2 \times 10^{25} \text{ W Hz}^{-1} \text{ sr}^{-1}$ (for Hubble constant $H_0 = 50 \text{ km s}^{-1} \text{ Mpc}^{-1}$), are edge-darkened (called type 1) in their brightness distribution, while all radio galaxies above this luminosity limit are more or less edge-brightened (called type 2). This correlation has withstood the test of time (Miley 1980; Antonucci 1993, 2012; Urry and Padovani 1995; Kembhavi and Narlikar 1999). However, because of a very strong redshift-luminosity correlation (Malmquist bias) in a flux-limited sample, like in the 3CR sample used by Fanaroff and Riley (1974), any effect related with redshift could appear as a luminosity-dependent effect and vice versa. This then begs a question – could all the morphological differences seen in FR 1 and 2 types of sources be primarily due to a transition across some critical redshift value, manifesting a cosmological evolutionary effect due to a critical ambient density value at that redshift, instead of, as almost universally believed, an effect of transition across a certain critical luminosity value?

Ashok K. Singal

Kamlesh Rajpurohit

¹Astronomy and Astrophysics Division, Physical Research Laboratory, Navrangpura, Ahmedabad - 380 009, India. Email:asingal@prl.res.in

²Thüringer Landessternwarte (TLS), Sternwarte 5, 07778 Tautenburg, Germany. Email : kamlesh@tls-tautenburg.de

Following the archetypal paper by Fanaroff and Riley (1974), where they first pointed out the presence of two distinct morphology types of radio galaxies in the strong source 3CR sample, ascribing the distinct morphology of each galaxy to its radio luminosity, it has ever since been thought to be only a luminosity-dependent effect (see e.g., Saripalli 2012 and the references therein). There have been no attempts to investigate the alternative possibility that it could as well be a redshift-dependent effect, and thereby demonstrating the strong evolution of source morphology with cosmic epoch. For instance, suppose one wants to explore a correlation of the morphology type of radio galaxies with redshift. Figure 1 shows a scatter plot with redshift and luminosity of both types of morphologies classified by Fanaroff and Riley (1974) in their sample. The demarcation is as good with redshift as it is with luminosity. It might be a moot point to guess what would have been the verdict, had Fanaroff and Riley in their seminal paper tried a correlation against only redshift, instead of luminosity. It is quite likely the effect then would have been interpreted as due to a very strong cosmological evolution with redshift, and the subsequent theoretical interpretations in that case perhaps very different.

The two scenarios have very different physical interpretations, and either could be of equal importance. For instance in the conventional interpretation, with intrinsic luminosities being the root cause of their different morphology types, there is a huge amount of literature about the relation between the luminosity break and the different morphology types (Saripalli 2012 and the references therein). In fact all the models and discussions in the literature currently available are almost exclusively only within that framework. On the other hand a definite correlation with redshift alone would imply that it is the cosmic evolution of the properties of sources (perhaps because of the ambient density falling below a certain critical value due to the Hubble expansion) that might give rise to these two different type of morphologies, with FR 1 type being the current favourite and the FR 2 type “a thing of past”.

All differences seen in FR 1 and FR 2 type sources, which are usually attributed to the differences in their luminosities, could as well be then related to the changing ambient densities with cosmic epoch. Also the very sharp division in luminosity could possibly be due to a critical ambient density value, which might divide the sources into two distinct morphology types. It might be the luminosity dependence or it might be the dependence on redshift that gives rise to these morphological differences, but this question could not be decisively settled based on any amount of arguments, sans actual

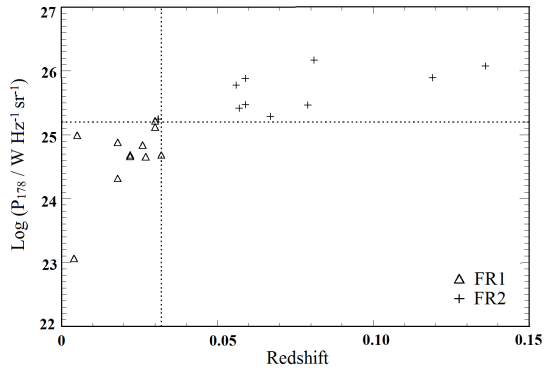


Fig. 1 A scatter plot of both types of FR morphologies (‘Δ’ for edge-darkened FR 1 type and ‘+’ for edge brightened FR 2 type) for the 3CR source sample of Fanaroff and Riley (1974) in the redshift-luminosity plane. To avoid undue compression of the scale, we have restricted the plot to a redshift limit of 0.15. There are no FR 1 type radio galaxies which lie beyond a redshift of 0.032 or have a luminosity $P_{178} > 2 \times 10^{25} \text{ W Hz}^{-1} \text{ sr}^{-1}$ (for $H_0 = 50 \text{ km s}^{-1} \text{ Mpc}^{-1}$) in the sample of Fanaroff and Riley

observational data. At least this particular aspect has not yet been investigated in the literature. We may add that there are reports of FR 1 types seen at redshifts larger than $z > 0.5$ (Saripalli et al. 2012), but a systematic investigation of this question is still needed using samples which are complete in the sense that all FR 1’s above the sensitivity limit of the sample are included.

2 The samples and the data

To make these investigations one needs sufficient data comprising sources at different flux-density levels, so that one could examine sources with similar luminosities at different redshifts as well as compare them at similar redshifts for different luminosities, thereby separating the two effects. We investigate this dependence of FR dichotomy of radio galaxies on luminosity and redshift by taking data from two such different samples. And since the transition value of luminosity or/and redshift may not be as sharp (see e.g., Baum et al. 1995 and the references therein) as inferred from the data used by Fanaroff and Riley (1974), we investigate the two effects by determining the median values of luminosity and redshift for FR 1 type sources in each one of our samples.

Our first sample is the 3CR (Laing et al. 1983), which is a complete strong source sample, with all necessary optical and radio information with good resolution maps so that one can in most cases unambigu-

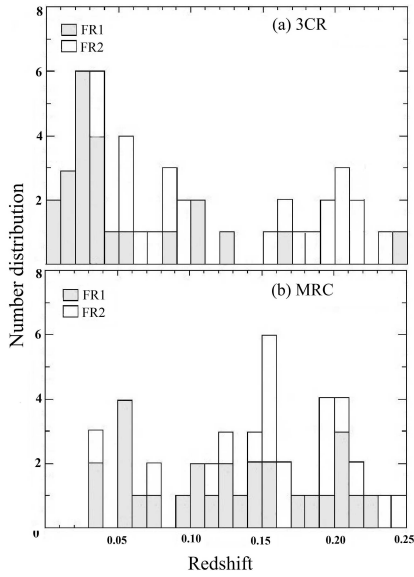


Fig. 2 Histograms showing distributions of FR 1/2 morphology types radio galaxies with redshift for the (a) 3CR and (b) MRC samples. It should be noted that all radio galaxies seen beyond the redshift limit of the plots (i.e. $z > 0.25$) are only of FR 2 type in both samples

ously decide the FR 1/2 type of morphologies. The sample is selected to include all radio sources with low-frequency (178 MHz) flux-density $S_{178} > 10.9$ Jy with declination $\delta > 10^\circ$ and the galactic latitude $b > 10^\circ$. The sample covers a solid angle of 4.23 steradian and contains a total of 173 sources. The updated data for the Laing et al. (1983) sample are available at <http://astroherzberg.org/people/chris-willott/research/3crr/>.

The second sample we have chosen is the essentially complete MRC (Molonglo Reference Catalog) sample (Kapahi et al. 1998) with $S_{408} \geq 0.95$ Jy in the declination range $-30^\circ < \delta < -20^\circ$, $b > 20^\circ$ but excluding the RA range $14^h 03^m - 20^h 20^m$. The MRC sample is about a factor ~ 5 or more deeper than the 3CR sample and has the required radio and optical information. The total sample comprises 550 sources, with 111 of them being quasars and the remainder radio galaxies. Optical identifications for the latter are complete up to a red magnitude of ~ 24 or a K magnitude of ~ 19 and among the still unidentified ones, which are expected to be at high redshifts $z \gtrsim 1$ and therefore of high luminosities as well, it is unlikely that there would be many FR 1 types.

To quantitatively distinguish between FR 1 and 2, following Fanaroff and Riley (1974), we classify a radio galaxy as FR 1 if the separation between the points of peak intensity in the two lobes is smaller than half the largest size of the source. Similarly FR 2 is the one

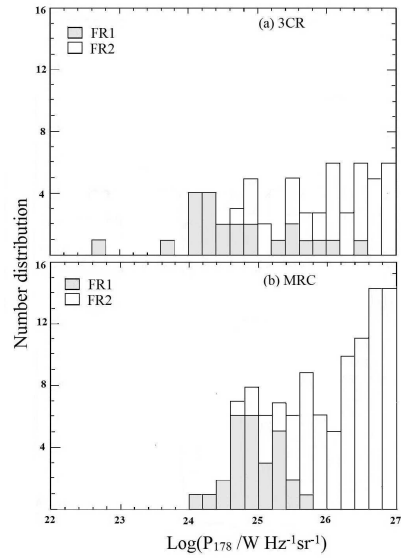


Fig. 3 Histograms showing distributions of FR 1/2 morphology types radio galaxies with radio luminosity (P_{178} in units of $\text{W Hz}^{-1} \text{sr}^{-1}$) for the (a) 3CR and (b) MRC samples. It should be noted that all radio galaxies seen beyond the luminosity limit of the plots (i.e. $P_{178} > 10^{27} \text{ W Hz}^{-1} \text{sr}^{-1}$) are only of FR 2 type in both samples

in which the separation between the points of peak intensity in the two lobes is greater than half the largest size of the source. This is equivalent to having the “hot spots” nearer to (FR 1) or further away from (FR 2) the central optical galaxy than the regions of diffuse radio emission. In both samples we have examined the radio maps and using the above criteria, we have classified each source into either of the two types (FR 1 and 2). There are a small number of sources that have an ambiguous FR classification. For example, there are sources of a hybrid type called HYMORS (one lobe of FR1 and the second of FR2 type (see, e.g., Gopal-Krishna and Wiita 2000)). Then there are some radio galaxies exhibiting two, or even three, pairs of lobes, where the AGN jet activity may have occurred more than once during a lifetime of a parent galaxy. These radio sources are called double-double radio galaxies (DDRGs), with some clear examples given by Saripalli, Subrahmanyan and Udaya Shankar (2002, 2003; also see Saikia and Jamrozny 2009). We excluded such cases where there was ambiguity in classifying them as FR1 or FR2. The number of such sources being relatively very small, it should not be too detrimental to our conclusions.

The luminosity of a source in our sample is calculated from its flux density S_{178} and the spectral index α ($S \propto$

Table 1 Percentile values of redshift and luminosity distributions for the FR 1 sources in the two samples.

Sample	$S_{178,med}$ (Jy)	Number FR 1	z_{med}	z_{lq}	z_{uq}	$\log(P_{178,med})$ (W Hz $^{-1}$ sr $^{-1}$)	$\log(P_{178,lq})$ (W Hz $^{-1}$ sr $^{-1}$)	$\log(P_{178,uq})$ (W Hz $^{-1}$ sr $^{-1}$)
3CR	19.4	23	0.03 ± 0.005	0.02	0.08	24.6 ± 0.2	24.2	25.5
MRC	2.7	27	0.12 ± 0.015	0.06	0.17	24.9 ± 0.1	24.6	25.2

$\nu^{-\alpha}$) as

$$P_{178} = S_{178} \mathcal{D}^2 (1+z)^{1+\alpha}, \quad (1)$$

where \mathcal{D} is the comoving cosmological distance calculated from the cosmological redshift z of the source. In general it is not possible to express \mathcal{D} in terms of z in a close-form analytical expression and one may have to evaluate it numerically. For example, in the flat universe models ($\Omega_m + \Omega_\Lambda = 1, \Omega_\Lambda \neq 0$), \mathcal{D} is given by (see e.g., Weinberg 2008),

$$\mathcal{D} = \frac{c}{H_0} \int_1^{1+z} \frac{dz}{(\Omega_\Lambda + \Omega_m z^3)^{1/2}}. \quad (2)$$

For a given Ω_Λ , \mathcal{D} can be evaluated from Eq. (2) by a numerical integration. Here Ω_m is the matter energy density (including that of the dark matter) and Ω_Λ is the vacuum energy (dark energy!) density, both defined in terms of the critical energy density $\Omega_c = 3H_0^2 c^2 / (8\pi G)$, where G is the gravitational constant and c is the velocity of light in vacuum. We have used $H_0 = 71 \text{ km s}^{-1} \text{ Mpc}^{-1}$, $\Omega_m = 0.27$ and $\Omega_\Lambda = 0.73$ (Spergel et al. 2003).

The detailed data used by us are given in Appendix, listed separately for both samples in Tables 2 and 3, which are self-explanatory.

3 Results and discussion

Figure 2 shows histograms of the distributions of radio galaxies with FR 1 type morphology against redshift for both our samples. We have restricted our plots to $z = 0.25$ only, as no FR 1 type radio galaxy is seen beyond this redshift in either sample. We have determined median value z_{med} for the redshift distribution of FR 1 sources for each sample. The details of the method for determining the median values and for the estimation of their rms errors are described in Singal (1988).

Figure 3 shows similar histograms of the distribution of radio galaxies with FR 1 type morphology against luminosity (at 178 MHz) for our two samples. Since all the FR 1's we are interested in are at low redshifts ($z < 0.25$), the specific cosmological parameters

do not make much difference for the luminosity evaluations except for the scaling factor due to the Hubble constant, which in our case makes luminosity estimates lower by a factor of $(71/50)^2 \approx 2$ than the calculations in Fanaroff and Riley (1974). Thus the FR 1/2 luminosity break of $P_{178} = 2 \times 10^{25} \text{ W Hz}^{-1} \text{ sr}^{-1}$ (for $H_0 = 50 \text{ km s}^{-1} \text{ Mpc}^{-1}$), arrived at by Fanaroff and Riley (1974) in their seminal paper, corresponds to $P_{178} = 10^{25} \text{ W Hz}^{-1} \text{ sr}^{-1}$ in our case. Again we have restricted our plots to $P_{178} = 10^{27} \text{ W Hz}^{-1} \text{ sr}^{-1}$ only, as no FR 1 type radio galaxy is seen beyond this luminosity value in either sample.

From Figure 3, it is also clear that the FR 1/2 break is not as sharp as stated in Fanaroff and Riley (1974), as some overlap of both type of morphologies is seen in luminosity. However there is no denying that in all samples there are only a few, if any, FR 1 types with luminosities $P_{178} > 10^{26} \text{ W Hz}^{-1} \text{ sr}^{-1}$.

In Table 1 we have listed the median values both for the redshift and the luminosity in each sample. Also listed are the median flux-density of FR 1's in each sample and the number of FR 1 sources in the sample. The rms error in z_{med} in each case is determined from the frequency distribution (histogram) of z -distribution. The rms error is given by $\sqrt{n}/(2f_p)$ in units of the class interval of z (Kendall 1945; Yule and Kendall 1950), where n is the total number of sources in the sample and f_p is the ordinate value of the smoothed frequency distribution at the median value in Figure 2. The median value of the distribution does seem to shift substantially with redshift for samples which differ in the median flux-density by a factor of ~ 7 . P_{med} and the rms error in P_{med} in each case is determined from the frequency distribution (histogram) of P -distribution in Figure 3, in the same way as for z_{med} as described above. Within errors there is hardly any difference in the two samples in the P_{med} value, which thus seems to be independent of the flux-density level of the sample. While the median value of redshift (z_{med}) for the weaker sample as compared to that of the stronger 3CR sample, differs by as much as a factor of about four, at about a 5σ level, the difference in the median value of luminosity (P_{med}) is only marginal, being only a factor of about $10^{0.3} \sim 2$ and that too within only about 1σ . From z_{med} and $\log(P_{med})$ values, it is clear that the FR 1 type of morphology of radio galaxies

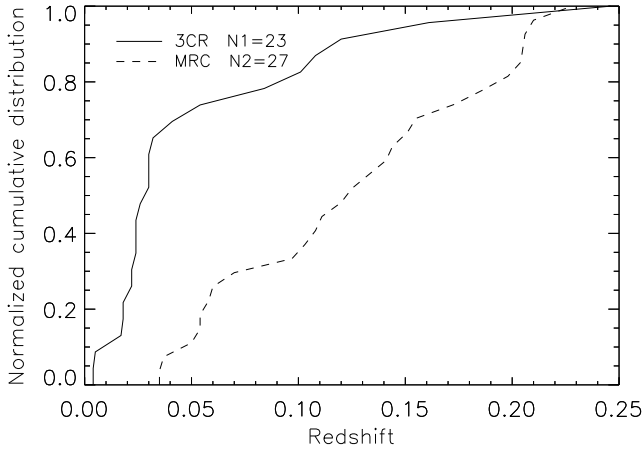


Fig. 4 Normalized cumulative distributions of FR 1 morphology type radio galaxies with redshift for the (a) 3CR sample (continuous curve) and (b) MRC sample (broken curve). N1 and N2 give the number of FR 1 radio galaxies in the 3CR and MRC samples, respectively

is indeed due to their luminosity below a critical value as indeed envisaged first time by Fanaroff and Riley (1974) and that it is not directly related to the redshift and hence not due to a cosmic evolution effect.

To ascertain it further we have examined the normalized cumulative distributions of FR 1 morphology type radio galaxies with redshift as well as luminosity. Figure 4 shows the normalized cumulative distributions of FR 1 morphology type radio galaxies with redshift for the two samples. Since the cumulative distributions shown are the normalized ones, therefore it automatically accounts for the fact that the sky coverages in the 3CR and MRC samples are different and we can directly compare the relative distributions of FR 1 types up to any given redshift, and thereby for the two corresponding different radio luminosity values in the two samples. If the morphology type depended only on redshift and not on luminosity, then both normalized cumulative distributions in Figure 4 should be more or less coincident, which definitely is not the case. In fact a Kolmogorov-Smirnov (K-S) test shows that the null-hypothesis that the two distribution are the same can be ruled out at a 99.99% confidence level.

In Table 1 we have listed, along with the median value (z_{med}), also the lower quartile (z_{lq}) and upper quartile (z_{uq}) of the cumulative distribution of the redshifts of the sources in these samples. We see that the space distribution of FR 1 morphology type radio galaxies does change with the flux-density levels of the sample. There is a large difference in the redshift distribution of the 3CR sample from those of the MRC sample. Note that the 3CR sample is about 7 times stronger in flux-density than the MRC sample. It seems that the

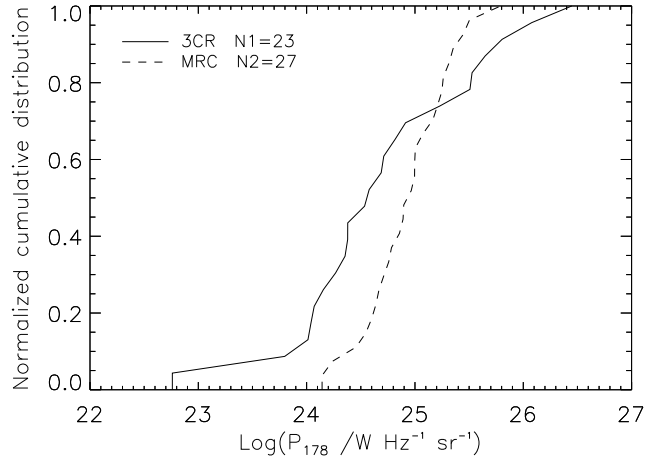


Fig. 5 Normalized cumulative distributions of FR 1 morphology type radio galaxies with radio luminosity (P_{178} in units of $\text{W Hz}^{-1} \text{sr}^{-1}$) for the (a) 3CR sample (continuous curve) and (b) MRC sample (broken curve). N1 and N2 give the number of FR 1 radio galaxies in the 3CR and MRC samples, respectively

redshift distribution of the FR 1 radio galaxies does depend on the flux-density level of the sample. Of course one may have to examine still weaker samples, where one might see FR 1 types $z > 0.25$, to see the generality of these results.

Figure 5 shows the normalized cumulative distribution of radio luminosity for FR 1 morphology type radio galaxies for both samples. The distributions overlap and there seems to be no gross difference in the luminosity distribution of FR 1 sources in the two samples. In Table 1 we have also listed the lower quartile (P_{lq}) and upper quartile (P_{uq}) of the cumulative distribution of the radio luminosity of the source in the two samples, which again are of very similar values. From these we find that half of FR 1 types lie in the narrow range of luminosities $P_{178} \sim 10^{24.7 \pm 0.5} \text{ W Hz}^{-1} \text{sr}^{-1}$, that is within a factor of 3 around $5 \times 10^{24} \text{ W Hz}^{-1} \text{sr}^{-1}$. Also all galaxies with radio luminosity above $P_{178} \sim 10^{26.5} \text{ W Hz}^{-1} \text{sr}^{-1}$ are only of type 2 with an edge brightened morphology. We have thus reaffirmed that the FR 1/2 dichotomy is due to a change in luminosity below and above a certain critical level, as first proposed by Fanaroff and Riley (1974) and followed in the literature ever since, and that it is not due to any cosmic epoch dependent evolution that gives rise to different FR 1 and 2 type morphologies.

Here we may add that the dual-population unification scheme (see e.g., Jackson & Wall 1999), where FR 1 and 2 type radio galaxies form two intrinsically distinct ‘unbeamed’ or ‘side-on’ parent populations of the steep spectrum extragalactic radio sources, has been running into serious problems as far as the FR 2 type

radio galaxy part is concerned. Unacceptably large mismatches with the predictions of the relative number and radio-size distributions of FR 2 radio galaxies and extended steep-spectrum quasars are seen in various redshift bins in different unbiased radio complete samples that have been examined (Singal & Singh 2013a, 2013b). There is almost complete absence of predicted foreshortening in the quasar radio sizes due to projection effects over and above the statistical spread. In the 3CR sample too, the predictions of unification scheme are not corroborated by the observed radio-size data even when the low-excitation radio galaxies from the FR 2 sample are excluded (Singal 2014). Except for that particular bin ($0.5 \leq z < 1$) of the 3CR sample, which incidentally was instrumental in the original proposition of the unification scheme (Barthel 1989), data in other redshift bins do not seem to yield the expected size ratios of FR 2 radio galaxies and quasars. It of course remains to be seen if the FR 1 type radio galaxy part of the dual-population unification scheme still holds true.

4 Conclusions

We have investigated if there is a direct dependence of the FR 1 and 2 morphology types of the radio galaxies on redshift. For this we compared their distributions in two different samples with different flux-density limits, which allowed us to separately study the effects of redshift and/or radio luminosity on the occurrences of the two morphology types. It was shown that the morphology type is not directly related to redshift and thereby not a cosmic epoch dependent effect. The break between the two types of morphologies seems to depend only upon the radio luminosity. Half of the FR 1 type radio galaxies lie in the narrow range of luminosities $P_{178} \sim 10^{24.7 \pm 0.5} \text{ W Hz}^{-1} \text{ sr}^{-1}$, with none exceeding the value $P_{178} \sim 10^{26.5} \text{ W Hz}^{-1} \text{ sr}^{-1}$, above which all were found to be exclusively type 2 with an edge brightened morphology.

ACKNOWLEDGEMENTS

KR expresses her gratitude to the Astronomy and Astrophysics Division of the Physical Research laboratory Ahmedabad, where work on this summer project was done under the guidance of AKS.

Appendix

Tables 2 and 3 give the radio and optical data used by us for the 3CR and MRC samples.

Table 2 : Radio and optical data for the 3CR sample

Source Name (1)	S_{178} (Jy) (2)	α (3)	FR Type (4)	z (5)	$\log(P_{178})$ (W Hz ⁻¹ sr ⁻¹) (6)
4C12.03	10.9	0.87	FR2	0.156	25.74
3C16	12.2	0.954	FR2	0.406	26.74
3C19	13.18	0.637	FR2	0.482	26.90
3C20	46.76	0.606	FR2	0.174	26.46
3C28	17.76	1.011	FR2	0.195	26.18
3C31	18.31	0.682	FR1	0.018	24.01
3C33	59.29	0.701	FR2	0.059	25.58
3C35	11.44	0.907	FR2	0.067	24.98
3C42	13.08	0.705	FR2	0.395	26.71
3C46	11.11	0.905	FR2	0.437	26.77
3C61.1	34	0.736	FR2	0.188	26.40
3C66B	26.81	0.736	FR1	0.022	24.35
3C76.1	13.29	0.588	FR1	0.032	24.38
3C83.1B	28.99	0.649	FR1	0.026	24.54
3C84	66.81	1.141	FR1	0.018	24.58
3C98	51.44	0.732	FR2	0.031	24.94
4C14.11	12.09	0.84	FR2	0.207	26.05
3C132	14.93	0.79	FR2	0.214	26.17
3C153	16.67	0.577	FR2	0.277	26.45
3C173.1	16.78	0.898	FR2	0.292	26.54
DA240	23.21	0.77	FR2	0.035	24.70
3C192	22.99	0.81	FR2	0.059	25.17
3C200	12.31	0.829	FR2	0.458	26.85
4C14.27	11.22	1.15	FR2	0.392	26.70
4C73.08	15.58	0.85	FR2	0.0581	24.98
3C264	28.34	0.82	FR1	0.022	24.38
3C272.1	21.14	0.6	FR1	0.004	22.76
A1552	12.53	0.94	FR1	0.084	25.23
3C274	1144.5	0.792	FR1	0.005	24.69
3C274.1	17.98	0.936	FR2	0.422	26.95
3C284	12.31	0.889	FR2	0.239	26.21
3C285	12.31	0.786	FR2	0.079	25.16
3C288	20.6	0.775	FR1	0.246	26.45
3C296	14.17	0.745	FR1	0.024	24.16
3C299	12.86	0.557	FR2	0.367	26.61
3C300	19.51	0.837	FR2	0.27	26.52
3C305	17.11	0.816	FR1	0.041	24.71
3C310	60.05	0.974	FR1	0.054	25.51
3C314.1	11.55	1.023	FR1	0.12	25.53
3C315	19.4	0.885	FR1	0.108	25.65

Table 2 – *continued*

Source Name (1)	S_{178} (Jy) (2)	α (3)	FR Type (4)	z (5)	$\log(P_{178})$ (W Hz ⁻¹ sr ⁻¹) (6)
3C319	16.67	0.852	FR2	0.192	26.12
3C321	14.71	0.825	FR2	0.096	25.42
3C326	22.23	0.88	FR2	0.088	25.52
NGC6109	11.66	0.76	FR1	0.03	24.27
3C338	51.12	1.074	FR1	0.03	24.91
3C341	11.77	0.863	FR2	0.448	26.81
NGC6251	10.9	0.72	FR1	0.024	24.04
3C346	11.88	0.807	FR1	0.161	25.80
3C349	14.49	0.739	FR2	0.205	26.12
3C381	18.09	0.729	FR2	0.16	25.98
3C388	26.81	0.683	FR2	0.09	25.61
3C401	22.78	0.635	FR2	0.201	26.29
3C433	61.25	0.719	FR1	0.101	26.08
3C436	19.4	0.855	FR2	0.214	26.29
3C438	48.72	0.822	FR2	0.29	26.99
3C449	12.53	0.742	FR1	0.017	23.80
3C452	59.29	0.825	FR2	0.081	25.87
NGC7385	11.66	0.75	FR1	0.024	24.07
3C457	14.27	1.229	FR2	0.428	26.91
3C465	41.2	0.833	FR1	0.03	24.82

Table 3 : Radio and optical data for the MRC sample

Source Name (1)	S_{408} (Jy) (2)	α (3)	FR Type (4)	z (5)	$\log(P_{178})$ (W Hz ⁻¹ sr ⁻¹) (6)
B0001-233	1.23	0.99	FR1	0.097	24.71
B0001-237	1.77	0.83	FR2	0.315	25.93
B0017-205	1.96	0.78	FR2	0.197	25.49
B0020-253	5.36	0.78	FR2	0.35	26.49
B0022-209	1.19	0.94	FR1	0.054	24.14
B0028-223	1.18	0.79	FR1	0.205	25.32
B0048-233	1.18	0.84	FR1	0.111	24.76
B0055-256	1.18	0.97	FR2	0.199	25.37
B0115-261	2.58	0.74	FR2	0.268	25.89
B0125-216	1.29	0.81	FR2	0.34	25.86
B0137-263	1.46	0.83	FR2	0.16	25.19
B0143-246	1.51	0.86	FR2	0.716	26.72
B0146-224	1.65	0.81	FR2	0.36	26.02
B0148-297	7.04	0.82	FR2	0.41	26.79
B0149-260	1.05	0.95	FR1	0.144	25.00
B0149-299	2.42	0.83	FR2	0.603	26.72
B0155-212	2.39	1.04	FR2	0.159	25.49
B0205-229	1.77	0.83	FR2	0.68	26.71
B0208-240	1.87	0.74	FR2	0.23	25.60
B0209-282	1.56	0.81	FR2	0.6	26.52
B0226-284	1.063	0.69	FR1	0.21	25.25
B0245-297	1.16	0.75	FR2	0.36	25.84
B0305-226	4.95	0.88	FR2	0.268	26.24
B0313-271	1.8	1.14	FR2	0.216	25.70
B0325-260	1.04	0.74	FR2	0.638	26.37
B0326-288	4.03	0.83	FR1	0.108	25.26
B0346-297	1.72	0.88	FR2	0.413	26.21
B0357-247	2.16	0.87	FR2	0.205	25.61
B0412-204	2.51	1	FR2	0.69	26.98
B0424-268	3.25	0.87	FR2	0.47	26.62
B0428-271	1.72	0.83	FR2	0.84	26.92
B0428-281	2.49	0.89	FR2	0.65	26.85
B0430-235	0.96	0.86	FR2	0.82	26.66
B0436-294	1.2	0.99	FR2	0.808	26.82
B0442-282	18.85	0.97	FR2	0.147	26.28
B0452-260	0.98	0.83	FR1	0.141	24.90
B0453-206	11.25	0.7	FR1	0.035	24.64
B0457-247	1.25	0.7	FR1	0.186	25.21
B0503-284	9	0.9	FR1	0.037	24.67
B0508-220	5.1	0.81	FR2	0.16	25.72

Table 3 – *continued*

Source Name (1)	S_{408} (Jy) (2)	α (3)	FR Type (4)	z (5)	$\log(P_{178})$ (W Hz ⁻¹ sr ⁻¹) (6)
B0512-200	0.98	0.69	FR1	0.133	24.78
B0522-239	1.08	0.8	FR2	0.5	26.17
B0529-210	1.33	0.96	FR2	0.42	26.16
B0541-243	3.61	0.98	FR2	0.523	26.83
B0602-289	1.37	1.03	FR2	0.56	26.51
B0938-205	1.35	0.88	FR2	0.371	26.00
B0952-224	1.71	0.62	FR1	0.228	25.50
B0959-225	1.04	0.68	FR2	0.895	26.67
B0959-263	1.72	0.82	FR2	0.677	26.69
B1006-214	1.35	0.78	FR2	0.246	25.55
B1006-286	3.54	0.76	FR2	0.582	26.81
B1023-226	1.08	0.94	FR2	0.586	26.41
B1025-270	1.82	0.83	FR2	0.72	26.79
B1026-202	1.95	0.88	FR2	0.566	26.59
B1027-225	1.11	1.1	FR2	0.15	25.12
B1029-233	1.08	0.86	FR2	0.611	26.41
B1033-251	1.53	0.83	FR2	0.44	26.20
B1036-215	0.98	0.82	FR2	0.585	26.30
B1048-238	1.31	0.76	FR1	0.206	25.35
B1056-272	0.97	0.97	FR2	0.25	25.50
B1103-244	3.9	0.97	FR1	0.05	24.60
B1126-246	1.1	0.74	FR1	0.155	25.00
B1126-290	2.42	0.74	FR2	0.41	26.28
B1129-250	0.98	0.91	FR2	1.065	26.98
B1136-211	1.1	1.02	FR2	0.87	26.88
B1222-252	1.82	0.99	FR2	0.077	24.67
B1226-211	3.28	0.8	FR2	0.191	25.70
B1240-209	4.58	0.87	FR2	0.42	26.65
B1251-289	4.22	1.2	FR1	0.058	24.86
B1257-253	1.5	0.68	FR1	0.06	24.24
B1303-215	1.46	0.76	FR1	0.12	24.89
B1309-211	1.67	0.83	FR2	0.3	25.86
B1313-248	2.14	0.9	FR2	0.74	26.93
B1325-257	1.16	0.93	FR2	0.62	26.49
B1343-253	1.05	0.74	FR2	0.129	24.81
B1346-252	1.27	1.26	FR1	0.125	25.07
B1358-214	1.48	1.08	FR2	0.5	26.45
B2020-211	1.59	1.43	FR1	0.054	24.46
B2038-280	1.47	1.23	FR2	0.39	26.26
B2039-236	1.63	0.86	FR2	0.621	26.60

Table 3 – *continued*

Source Name (1)	S_{408} (Jy) (2)	α (3)	FR Type (4)	z (5)	$\log(P_{178})$ (W Hz ⁻¹ sr ⁻¹) (6)
B2040-219	1.2	1.08	FR1	0.204	25.45
B2045-245	1.99	1	FR2	0.73	26.94
B2053-201	6.37	0.8	FR2	0.155	25.79
B2057-286	2.34	0.93	FR2	0.605	26.77
B2101-214	0.96	0.73	FR1	0.198	25.17
B2104-256	28.1	0.79	FR2	0.037	25.12
B2116-250	1.74	0.89	FR2	0.467	26.35
B2117-269	2.6	0.77	FR1	0.103	25.00
B2118-266	1.17	0.58	FR2	0.343	25.71
B2132-236	0.95	0.95	FR2	0.81	26.70
B2134-281	2.12	0.73	FR1	0.07	24.55
B2137-279	1.21	0.94	FR2	0.64	26.55
B2148-228	1.42	0.99	FR2	0.85	26.95
B2206-251	2.04	0.93	FR2	0.158	25.36
B2226-224	1.25	0.89	FR2	0.38	26.00
B2236-264	1.23	0.83	FR2	0.43	26.08
B2254-248	1.81	0.68	FR2	0.54	26.40
B2256-207	1.21	1.02	FR2	0.87	26.93
B2308-214	0.99	0.83	FR1	0.151	24.97
B2311-222	2.24	0.78	FR2	0.434	26.33
B2313-277	1.9	0.97	FR2	0.614	26.72
B2317-277	5.44	0.73	FR1	0.173	25.79
B2321-228	1.03	1.21	FR2	0.114	24.87
B2324-259	1.44	0.72	FR2	0.286	25.69
B2325-213	3.07	0.94	FR2	0.58	26.85
B2343-243	1.85	0.8	FR2	0.6	26.59
B2348-235	1.47	0.83	FR2	0.952	26.98

References

- Antonucci, R. 1993, ARAA, 31, 473
Antonucci, R. 2012, Astr. Astrophys. Trans., 4, 557
Barthel, P. D. 1989, ApJ, 336, 606
Baum, A. A., Zirbel, E. L., O'Dea, P. 1995, ApJ, 451, 88
Fanaroff B. L., Riley J. M. 1974, MNRAS, 167, 31P
Gopal-Krishna, Wiita, P. J. 2000, A&A, 363, 507
Jackson, C. A., Wall, J. V. 1999, MNRAS, 304, 160
Kapahi, V. K., Athreya, R. M., van Breugel, W., McCarthy, P. J., Subrahmanya, C. R. 1998, ApJS, 118, 275.
Kembhavi, A. K., Narlikar, J. V. 1999, Quasars and Active Galactic Nuclei – An Introduction (Cambridge: Camb. Univ.), 357
Kendall, M. G. 1945, The Advanced Theory of Statistics, vol. 1 (London: Charles Griffin), 211
Laing R. A., Riley J. M., Longair M. S. 1983, MNRAS, 204, 151
Miley, G. K. 1980, ARAA, 18, 165
Saikia, D. J., and Jamrozy, M. 2009, BASI, 37, 63
Saripalli, L. 2012, AJ, 144, 85
Saripalli, L., Subrahmanyan, R., Thorat, K. et al. 2012, ApJS, 199, 27
Saripalli, L., Subrahmanyan, R., Udaya Shankar, N. 2002, ApJ, 565, 256
Saripalli, L., Subrahmanyan, R., Udaya Shankar, N. 2003, ApJ, 590, 181
Singal A. K. 1988, MNRAS, 233, 87
Singal A. K. 2014, AJ, 148, 16
Singal, A. K., Singh, R. L. 2013a, ApJ 766, 37
Singal, A. K., Singh, R. L. 2013b, MNRAS, 435, L38
Spergel, D. N., Verde, L., Peiris, H. V. et al. 2003, ApJS, 148, 175
Urry, C. M., Padovani, P. 1995, PASP, 107, 803
Weinberg, S. 2008, Cosmology (Oxford: Oxford Univ.), 43
Yule, U. G., Kendall, M. G. 1950, An Introduction to the Theory of Statistics (London: Charles Griffin), 425